

Proceedings of the 12th International Conference on
Computational Fluid Dynamics in the Oil & Gas,
Metallurgical and Process Industries

Progress in Applied CFD – CFD2017



SINTEF Proceedings

Editors:

Jan Erik Olsen and Stein Tore Johansen

Progress in Applied CFD – CFD2017

Proceedings of the 12th International Conference on Computational Fluid Dynamics
in the Oil & Gas, Metallurgical and Process Industries

SINTEF Academic Press

SINTEF Proceedings no 2

Editors: Jan Erik Olsen and Stein Tore Johansen

Progress in Applied CFD – CFD2017

Selected papers from 10th International Conference on Computational Fluid Dynamics in the Oil & Gas, Metallurgical and Process Industries

Key words:

CFD, Flow, Modelling

Cover, illustration: Arun Kamath

ISSN 2387-4295 (online)

ISBN 978-82-536-1544-8 (pdf)

© Copyright SINTEF Academic Press 2017

The material in this publication is covered by the provisions of the Norwegian Copyright Act. Without any special agreement with SINTEF Academic Press, any copying and making available of the material is only allowed to the extent that this is permitted by law or allowed through an agreement with Kopinor, the Reproduction Rights Organisation for Norway. Any use contrary to legislation or an agreement may lead to a liability for damages and confiscation, and may be punished by fines or imprisonment

SINTEF Academic Press

Address: Forskningsveien 3 B
 PO Box 124 Blindern
 N-0314 OSLO

Tel: +47 73 59 30 00

Fax: +47 22 96 55 08

www.sintef.no/byggforsk

www.sintefbok.no

SINTEF Proceedings

SINTEF Proceedings is a serial publication for peer-reviewed conference proceedings on a variety of scientific topics.

The processes of peer-reviewing of papers published in SINTEF Proceedings are administered by the conference organizers and proceedings editors. Detailed procedures will vary according to custom and practice in each scientific community.

PREFACE

This book contains all manuscripts approved by the reviewers and the organizing committee of the 12th International Conference on Computational Fluid Dynamics in the Oil & Gas, Metallurgical and Process Industries. The conference was hosted by SINTEF in Trondheim in May/June 2017 and is also known as CFD2017 for short. The conference series was initiated by CSIRO and Phil Schwarz in 1997. So far the conference has been alternating between CSIRO in Melbourne and SINTEF in Trondheim. The conferences focuses on the application of CFD in the oil and gas industries, metal production, mineral processing, power generation, chemicals and other process industries. In addition pragmatic modelling concepts and bio-mechanical applications have become an important part of the conference. The papers in this book demonstrate the current progress in applied CFD.

The conference papers undergo a review process involving two experts. Only papers accepted by the reviewers are included in the proceedings. 108 contributions were presented at the conference together with six keynote presentations. A majority of these contributions are presented by their manuscript in this collection (a few were granted to present without an accompanying manuscript).

The organizing committee would like to thank everyone who has helped with review of manuscripts, all those who helped to promote the conference and all authors who have submitted scientific contributions. We are also grateful for the support from the conference sponsors: ANSYS, SFI Metal Production and NanoSim.

Stein Tore Johansen & Jan Erik Olsen



Organizing committee:

Conference chairman: Prof. Stein Tore Johansen

Conference coordinator: Dr. Jan Erik Olsen

Dr. Bernhard Müller

Dr. Sigrid Karstad Dahl

Dr. Shahriar Amini

Dr. Ernst Meese

Dr. Josip Zoric

Dr. Jannike Solsvik

Dr. Peter Witt

Scientific committee:

Stein Tore Johansen, SINTEF/NTNU

Bernhard Müller, NTNU

Phil Schwarz, CSIRO

Akio Tomiyama, Kobe University

Hans Kuipers, Eindhoven University of Technology

Jinghai Li, Chinese Academy of Science

Markus Braun, Ansys

Simon Lo, CD-adapco

Patrick Segers, Universiteit Gent

Jiyuan Tu, RMIT

Jos Derksen, University of Aberdeen

Dmitry Eskin, Schlumberger-Doll Research

Pär Jönsson, KTH

Stefan Pirker, Johannes Kepler University

Josip Zoric, SINTEF

CONTENTS

PRAGMATIC MODELLING	9
On pragmatism in industrial modeling. Part III: Application to operational drilling	11
CFD modeling of dynamic emulsion stability	23
Modelling of interaction between turbines and terrain wakes using pragmatic approach	29
FLUIDIZED BED	37
Simulation of chemical looping combustion process in a double looping fluidized bed reactor with cu-based oxygen carriers.....	39
Extremely fast simulations of heat transfer in fluidized beds.....	47
Mass transfer phenomena in fluidized beds with horizontally immersed membranes	53
A Two-Fluid model study of hydrogen production via water gas shift in fluidized bed membrane reactors	63
Effect of lift force on dense gas-fluidized beds of non-spherical particles	71
Experimental and numerical investigation of a bubbling dense gas-solid fluidized bed	81
Direct numerical simulation of the effective drag in gas-liquid-solid systems	89
A Lagrangian-Eulerian hybrid model for the simulation of direct reduction of iron ore in fluidized beds.....	97
High temperature fluidization - influence of inter-particle forces on fluidization behavior	107
Verification of filtered two fluid models for reactive gas-solid flows	115
BIOMECHANICS.....	123
A computational framework involving CFD and data mining tools for analyzing disease in carotid artery	125
Investigating the numerical parameter space for a stenosed patient-specific internal carotid artery model.....	133
Velocity profiles in a 2D model of the left ventricular outflow tract, pathological case study using PIV and CFD modeling.....	139
Oscillatory flow and mass transport in a coronary artery.....	147
Patient specific numerical simulation of flow in the human upper airways for assessing the effect of nasal surgery.....	153
CFD simulations of turbulent flow in the human upper airways	163
OIL & GAS APPLICATIONS	169
Estimation of flow rates and parameters in two-phase stratified and slug flow by an ensemble Kalman filter	171
Direct numerical simulation of proppant transport in a narrow channel for hydraulic fracturing application	179
Multiphase direct numerical simulations (DNS) of oil-water flows through homogeneous porous rocks	185
CFD erosion modelling of blind tees	191
Shape factors inclusion in a one-dimensional, transient two-fluid model for stratified and slug flow simulations in pipes	201
Gas-liquid two-phase flow behavior in terrain-inclined pipelines for wet natural gas transportation	207

NUMERICS, METHODS & CODE DEVELOPMENT	213
Innovative computing for industrially-relevant multiphase flows	215
Development of GPU parallel multiphase flow solver for turbulent slurry flows in cyclone.....	223
Immersed boundary method for the compressible Navier–Stokes equations using high order summation-by-parts difference operators	233
Direct numerical simulation of coupled heat and mass transfer in fluid-solid systems	243
A simulation concept for generic simulation of multi-material flow, using staggered Cartesian grids.....	253
A cartesian cut-cell method, based on formal volume averaging of mass, momentum equations.....	265
SOFT: a framework for semantic interoperability of scientific software	273
 POPULATION BALANCE	 279
Combined multifluid-population balance method for polydisperse multiphase flows	281
A multifluid-PBE model for a slurry bubble column with bubble size dependent velocity, weight fractions and temperature.....	285
CFD simulation of the droplet size distribution of liquid-liquid emulsions in stirred tank reactors	295
Towards a CFD model for boiling flows: validation of QMOM predictions with TOPFLOW experiments	301
Numerical simulations of turbulent liquid-liquid dispersions with quadrature-based moment methods.....	309
Simulation of dispersion of immiscible fluids in a turbulent couette flow	317
Simulation of gas-liquid flows in separators - a Lagrangian approach.....	325
CFD modelling to predict mass transfer in pulsed sieve plate extraction columns	335
 BREAKUP & COALESCENCE	 343
Experimental and numerical study on single droplet breakage in turbulent flow	345
Improved collision modelling for liquid metal droplets in a copper slag cleaning process	355
Modelling of bubble dynamics in slag during its hot stage engineering.....	365
Controlled coalescence with local front reconstruction method	373
 BUBBLY FLOWS	 381
Modelling of fluid dynamics, mass transfer and chemical reaction in bubbly flows	383
Stochastic DSMC model for large scale dense bubbly flows.....	391
On the surfacing mechanism of bubble plumes from subsea gas release.....	399
Bubble generated turbulence in two fluid simulation of bubbly flow	405
 HEAT TRANSFER	 413
CFD-simulation of boiling in a heated pipe including flow pattern transitions using a multi-field concept	415
The pear-shaped fate of an ice melting front	423
Flow dynamics studies for flexible operation of continuous casters (flow flex cc).....	431
An Euler-Euler model for gas-liquid flows in a coil wound heat exchanger.....	441
 NON-NEWTONIAN FLOWS.....	 449
Viscoelastic flow simulations in disordered porous media	451
Tire rubber extrudate swell simulation and verification with experiments	459
Front-tracking simulations of bubbles rising in non-Newtonian fluids.....	469
A 2D sediment bed morphodynamics model for turbulent, non-Newtonian, particle-loaded flows.....	479

METALLURGICAL APPLICATIONS.....	491
Experimental modelling of metallurgical processes	493
State of the art: macroscopic modelling approaches for the description of multiphysics phenomena within the electroslag remelting process	499
LES-VOF simulation of turbulent interfacial flow in the continuous casting mold	507
CFD-DEM modelling of blast furnace tapping	515
Multiphase flow modelling of furnace tapholes	521
Numerical predictions of the shape and size of the raceway zone in a blast furnace.....	531
Modelling and measurements in the aluminium industry - Where are the obstacles?	541
Modelling of chemical reactions in metallurgical processes.....	549
Using CFD analysis to optimise top submerged lance furnace geometries	555
Numerical analysis of the temperature distribution in a martensitic stainless steel strip during hardening.....	565
Validation of a rapid slag viscosity measurement by CFD.....	575
Solidification modeling with user defined function in ANSYS Fluent.....	583
Cleaning of polycyclic aromatic hydrocarbons (PAH) obtained from ferroalloys plant.....	587
Granular flow described by fictitious fluids: a suitable methodology for process simulations	593
A multiscale numerical approach of the dripping slag in the coke bed zone of a pilot scale Si-Mn furnace.....	599
INDUSTRIAL APPLICATIONS	605
Use of CFD as a design tool for a phosphoric acid plant cooling pond	607
Numerical evaluation of co-firing solid recovered fuel with petroleum coke in a cement rotary kiln: Influence of fuel moisture	613
Experimental and CFD investigation of fractal distributor on a novel plate and frame ion-exchanger	621
COMBUSTION	631
CFD modeling of a commercial-size circle-draft biomass gasifier.....	633
Numerical study of coal particle gasification up to Reynolds numbers of 1000.....	641
Modelling combustion of pulverized coal and alternative carbon materials in the blast furnace raceway	647
Combustion chamber scaling for energy recovery from furnace process gas: waste to value	657
PACKED BED.....	665
Comparison of particle-resolved direct numerical simulation and 1D modelling of catalytic reactions in a packed bed	667
Numerical investigation of particle types influence on packed bed adsorber behaviour	675
CFD based study of dense medium drum separation processes	683
A multi-domain 1D particle-reactor model for packed bed reactor applications.....	689
SPECIES TRANSPORT & INTERFACES	699
Modelling and numerical simulation of surface active species transport - reaction in welding processes	701
Multiscale approach to fully resolved boundary layers using adaptive grids.....	709
Implementation, demonstration and validation of a user-defined wall function for direct precipitation fouling in Ansys Fluent.....	717

FREE SURFACE FLOW & WAVES	727
Unresolved CFD-DEM in environmental engineering: submarine slope stability and other applications.....	729
Influence of the upstream cylinder and wave breaking point on the breaking wave forces on the downstream cylinder	735
Recent developments for the computation of the necessary submergence of pump intakes with free surfaces	743
Parallel multiphase flow software for solving the Navier-Stokes equations	752
 PARTICLE METHODS	 759
A numerical approach to model aggregate restructuring in shear flow using DEM in Lattice-Boltzmann simulations	761
Adaptive coarse-graining for large-scale DEM simulations.....	773
Novel efficient hybrid-DEM collision integration scheme.....	779
Implementing the kinetic theory of granular flows into the Lagrangian dense discrete phase model.....	785
Importance of the different fluid forces on particle dispersion in fluid phase resonance mixers	791
Large scale modelling of bubble formation and growth in a supersaturated liquid.....	798
 FUNDAMENTAL FLUID DYNAMICS	 807
Flow past a yawed cylinder of finite length using a fictitious domain method	809
A numerical evaluation of the effect of the electro-magnetic force on bubble flow in aluminium smelting process.....	819
A DNS study of droplet spreading and penetration on a porous medium.....	825
From linear to nonlinear: Transient growth in confined magnetohydrodynamic flows.....	831

VALIDATION OF A RAPID SLAG VISCOSITY MEASUREMENT BY CFD

B. Vandensande, E. Nagels*, S. Arnout

InsPyro, Kapeldreef 60, 3001 Leuven, Belgium

* E-mail: els.nagels@inspyro.be

ABSTRACT

Slag viscosity is an important property in daily process practice, as well as for modelling flows in metallurgical processes accurately. Measuring slag viscosities is a challenging task, and usually requires a specific high-temperature furnace set-up, which needs to be gas tight and still allow for e.g. torque measurements on a well-aligned rotating viscometer spindle. The inclined plane technique is an alternative, requiring little time and no complex instruments. A slag sample, heated in a crucible or from an industrial furnace, is poured onto an inclined steel plate, and runs down while solidifying, to form a ribbon of a certain length. The ribbon length has been experimentally proven to be correlated rather accurately to the high temperature viscosity. However, as the viscosity increases sharply during cooling, the ribbon length should also depend on the temperature dependence of the viscosity. To study these effects, a CFD model has been built in this project. This model also allows to understand the effect of slag weight, steel plate thickness, temperature, and inclination, which could influence the results. The model is based on a VOF description for the slag surface and uses accurate heat capacity and viscosity functions based on thermodynamic calculations. This approach allows to increase the reliability of the fast slag viscosity measurement.

Keywords: CFD, metallurgy, viscosity, slag

NOMENCLATURE.

Greek Symbols

- α Angle of inclined plane, [°] or Volume fraction, [-].
 Γ Diffusion coefficient, [m²/s].
 η Viscosity, [Pa s] or [Poise].
 ρ Mass density, [kg/m³].
 ϕ A conserved scalar

Latin Symbols

- A Parameter of Wayman-Frenkel relationship, [Pa.s/K].
B Parameter of Wayman-Frenkel relationship, [K].
 c_p Heat capacity, [J/kg.K]
L Ribbon length, [m].
 \dot{m}_{pq} Mass transfer from phase p to phase q, [kg/m³].
 n Number of phases, [-].
 S_ϕ A source term of conserved scalar ϕ

- T Temperature, [K] or [°C].
 \mathbf{v} Velocity, [m/s].
X Molecular fraction, [-].

Sub/superscripts

- p Phase p.
q Phase q.

INTRODUCTION

Within the metal producing industry, slag control is often instrumental for the efficiency of the production. Controlling the slag composition is key to have a good metal yield in any smelting or refining activity (Reis, 2014). Next to composition, which defines the chemical equilibria of reactions, also the physical property viscosity has a direct impact on the production process. To remove a slag from the furnace, it is commonly tapped as a liquid. This procedure requires a slag with a low viscosity, allowing it to flow. A low viscosity has the additional advantage that the metal-slag reactions will encounter less kinetic difficulties, e.g. due to better mixing. However, a low viscosity slag with a high reactivity towards the furnace lining could accelerate the refractory wear (Chen, 2016). Viscosity is thus a very important, although hard to measure, property of the slag. This research project explores the possibilities of an experimental measurement called the inclined plane technique. The measurement is tested in a lab environment and is modelled by CFD, which allows for a sensitivity analysis. It is clear that when this technique is installed in an industrial environment, some initial validation is needed. From this study with both CFD and experiments, a first indication of the most influential parameters is obtained.

MODEL DESCRIPTION

Inclined plane technique

The inclined plane technique is a relatively simple and robust set-up. This gives the opportunity to use the measurement both in industrial as well as in lab environments. In this method, a certain amount of a slag is placed in a graphite or platinum crucible and heated to a temperature above the melting temperature. Industrially, it can be taken directly from the furnace or from the slag stream during tapping. The molten slag is then quickly poured onto a V-shaped stainless steel plate, set at a certain inclination (the inclined plane).

The slag flows down the inclined plane until it solidifies and forms a slag ribbon. The experimental set-up used by Dey and Riaz (2012) is shown in Figure 1. The length of the slag ribbon (L) has been found to be exponentially related to the viscosity (η) (Dey, 2012; Mills, 1997). To estimate the slag viscosity by the Inclined Plane Method, a (L , η) curve must be constructed first. The (L , η) curve can be constructed experimentally by measuring the ribbon length of slags with known viscosities. Subsequently, when the (L , η) curve is available, a slag sample with unknown viscosity is poured and then its ribbon length is measured. With the measured ribbon length and the available (L , η) curve, the viscosity of the studied slag can be estimated. This gives a quantitative technique to evaluate the flow properties of slag.

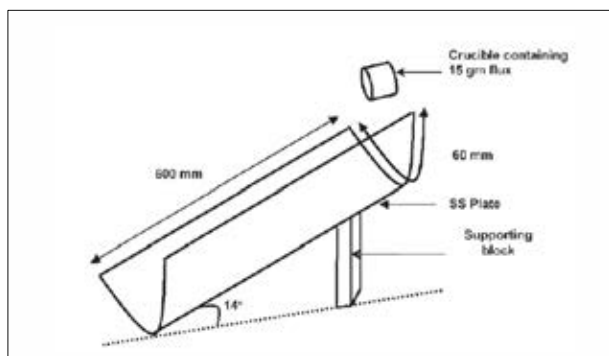


Figure 1: Schematic representation of set-up for the inclined plane technique (After Dey, 2012)

The experimental technique was evaluated and proven to be a fast technique with a good repeatability of the results. In this experimental phase, the angle of the set-up, the amount of material and initial temperature were considered as parameters, as shown in Table 1. Complementing this, the aim of the CFD calculations is to evaluate the robustness of the technique towards the experimental parameters, and towards parameters which are harder to vary experimentally, such as the thickness of the inclined plate, the temperature dependence of the viscosity and the initial temperature of this plate.

Table 1: Experimental parameters

Series	T(°C)	Inclination	Mass of slag	Composition
1	1300	12.5°	15g	1-6
2	1350	12.5°	15g	1-6
3	1400	12.5°	15g	1-6
4	1300	25°	15g	1-3
5	1300	12.5°	30g	1-3

Viscosity model

In literature, several models are described for the viscosity of a slag as a function of composition and temperature. In general, slags are formed by a solution of oxides and silicates. For the sake of viscosity, generally three types of oxides, namely acidic oxides, basic oxides and amphoteric oxides, are considered (Slag Atlas, 1995).



Figure 2: Picture of the experimental set-up

Acidic oxides such as SiO_2 , P_2O_5 , B_2O_3 possess stiff, highly covalent metal-oxygen bonds. SiO_2 forms tetrahedral anionic molecules of SiO_4^{4-} (silicate) which polymerize with each other to form more complicated polymer structures and even 3D networks, leading to high viscosities (Slag Atlas, 1995 and Kekkonen, 2012). With addition of basic oxides such as CaO , Na_2O , MgO with ionic metal-oxygen bonds, which do not require defined bond angles, the network breaks down, and consequently the viscosity of the slag decreases. The magnitude of the network-breaking effect depends strongly on the components and their proportions present in the slag. Amphoteric oxides, such as Al_2O_3 , Fe_2O_3 , may act either as a network former or a breaker, depending on the composition of the slag (Kekkonen, 2012).

The temperature dependence of slag viscosity is mostly expressed in the form of the Wayman-Frenkel relationship (Equation 1) in which A and B are viscosity parameters and T is the temperature in K.

Wayman-Frenkel relationship

$$\eta = AT \exp\left(\frac{B}{T}\right) \quad (1)$$

CFD model specifications

Geometry and mesh of 2D model

The flow of the liquid slag in a V-shaped gutter is simplified to a 2D geometry to decrease the calculation time. The third dimension is modelled as a symmetry plane which corresponds with an infinite long plate over which a wave of liquid slag flows. Clearly, this has consequences for the cooling of the slag which will be discussed further when comparing the 2D to 3D situation. For now, the aim is to verify the influence of some parameters on the length of the formed ribbon which can qualitatively be understood from the 2D case. The mesh contains 30668 quad elements. A small cell size of $2.5 \cdot 10^{-7} \text{ m}^2$ and 2nd order upwind schemes are used to capture the strong temperature and viscosity gradients present. The steel plate is meshed as well to capture the heat transfer in the solid domain. The mesh dependency of the ribbon length is illustrated in Table 2. A variation of -6% in the final ribbon length is significant and indicates that mesh effects are present. However, these deviations are within the experimental error margin.

Table 2: Validation of mesh dependency

Series	Mesh elements [-]	Final ribbon length [m]
1	13137	0,1577
2	30668	0,1547
3	54627	0,1449

Governing equations

Modelling the inclined plane technique is a multiphase problem with steep viscosity and temperature gradients. By using the volume of fluid (VOF) approach only one set of continuity equations must be solved for each iteration (Ansys, 2017). In its most general form the conservation of a scalar can be written as in Equation 2 (Ferziger, 2002 and Versteeg, 2007).

General transport equation

$$\frac{\partial \rho \phi}{\partial t} + \text{div}(\rho \phi \mathbf{v}) = \text{div}(\Gamma \text{grad} \phi) + S_{\phi} \quad (2)$$

with \mathbf{v} the velocity vector, S_{ϕ} the source term of conserved parameter ϕ and Γ the diffusion coefficient. The conserved variable ϕ can be taken equal to 1, equal to the velocity in x, y, z direction or equal to the temperature. The conservation equations of mass, x-momentum, y-momentum, z-momentum or energy will be found respectively (Versteeg, 2007). Equation 3 gives as an example the continuity equation for mass conservation.

Continuity equation

$$\frac{\partial \rho}{\partial t} + \text{div}(\rho \mathbf{v}) = \text{div}(\Gamma \text{grad}(1)) + S_{\phi} = 0 \quad (3)$$

Additionally, in the Eulerian VOF description the interface is tracked by solving an additional continuity equation of the volume fraction for one or more phases (Ansys, 2017). The continuity equation for phase q in a simulation with n phases is given in Equation 4 (Ansys, 2017).

$$\frac{1}{\rho_q} \left[\frac{\partial \rho_q \alpha_q}{\partial t} + \text{div}(\rho_q \alpha_q \mathbf{v}_q) \right] = \frac{1}{\rho_q} \left[\sum_{p=1}^n (\dot{m}_{pq} - \dot{m}_{qp}) + S_{\alpha q} \right] \quad (4)$$

with \dot{m}_{pq} being the mass transfer from phase p to phase q . The interface is reconstructed from the volume fractions. For this model the Compressive Interface Capturing Scheme for Arbitrary Meshes (CISAM) is used due to its ability to cope with large differences in viscosity (Ansys, 2017).

Material properties and boundary conditions

The material properties used in the CFD model are given in Table 3 (Ansys, 2017 and Bale et al., 2016 and Slag Atlas, 1995). The slag properties correspond to the reference slag M1 of Dey and Riaz (2012).

Table 3: Material properties used for modelling

Property	Air	Slag	Steel
c_p [J/kgK]	1006	1273	502
ρ [kg/m ³]	1.225	2580	8030
α [W/mK]	0.024	0.8	16.3
σ [N/m]	-	0.4 (with air)	-
η [Pa.s]	$1.78 \cdot 10^{-5}$	UDF (see below)	-

The viscosity of the slag phase is implemented in Fluent 18.0 using a user defined function (UDF). The temperature dependence of the viscosity is calculated with the Riboud model. This model gives the coefficients of the Wayman-Frenkel relation based on the composition for the slag (Slag Atlas, 1995). These estimated coefficients are then used in the UDF to calculate the viscosity in each cell depending on the cell temperature. The viscosity calculated by the UDF is limited to 1000 Pa.s. This limitation is necessary to avoid the extreme gradients for lower temperatures. Without this limitation, the viscosities predicted by the Wayman-Frenkel equation cause the solver to diverge. This behaviour is observed for both the 2D and 3D situation. A limit of 1000 Pa.s is not expected to have an influence on the end result as the achieved solution displays no further movement of the slag.

The outer walls of the solid domain (steel plate) are modelled by a convection wall with a heat transfer coefficient of 15 W/(m²K) and a free stream temperature of 21 °C. The outer walls of the fluid domain are set to a fixed temperature of 21 °C. In the contact area between liquid and solid, the temperatures are coupled. ‘‘No slip’’ boundaries are used on all boundaries of the fluid domain.

The initial parameters of the base case are given in Table 4. The inclination is implemented by the orientation of the gravity. This allows the inclination to be changed more easily because the world reference and mesh can remain the same. The initial slag area corresponds to a cross section of the 3D case with 15g of slag.

Table 4: Initial conditions of base case

Inclination	12.5°
Initial temperature of steel plate	21°C
Initial temperature of air	21°C
Initial temperature of slag	1300°C
Initial area of slag	$48.1 \cdot 10^{-6}$ m ²
Time step	0.0005s (except first 1000 iterations where it is 0.0001s)

In the experiments, the slag solidifies when it runs down the plate. In the simulations, the slag is said to be solidified when the slag ribbon length remains constant for at least one second.

RESULTS

Inclined plane technique test results

It is expected that the temperature of the liquid slag has a direct influence on the slag viscosity following the Wayman-Frenkel relation. In the experiments, it is indeed seen that a higher initial temperature results in a longer ribbon length (Figure 3). The compositions in Figure 3 correspond to earlier work by Dey and Riaz (2012). For all tested compositions, the influence of temperature seems to have an equal effect. From Figure 4, it is learned that the initial temperature has no influence on the relation between ribbon length and the viscosity, indicating that temperature information is not necessary to measure the viscosity with this technique. This means, the technique can be used to measure the viscosity at any experimental temperature, without knowing the temperature.

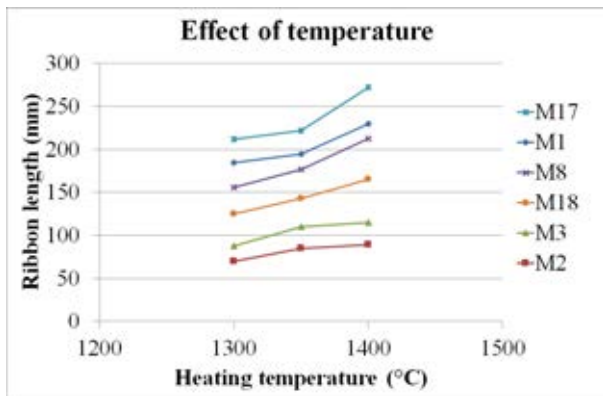


Figure 3: Increasing the initial temperature results in a larger ribbon length, corresponding to the viscosity dependence on temperature and composition

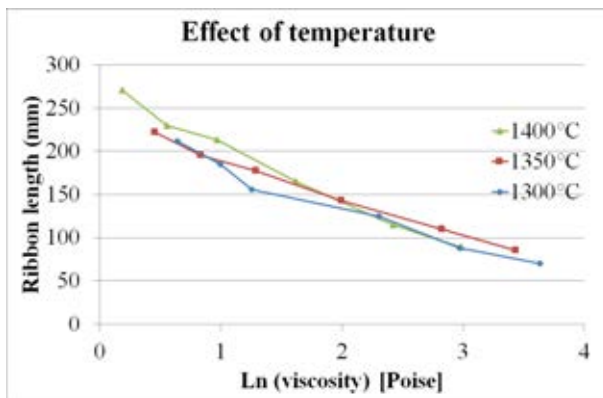


Figure 4: Ribbon length displays a linear relation with the logarithm of the viscosity over different initial temperatures

The second slag-related parameter for this test is the amount of material used for the inclined plane measurement. Obviously, when more material is present, a longer ribbon is expected. For three compositions, tests with both 15 g and 30 g are performed. An overview of the resulting ribbon lengths is given in Figure 5. These results indicate that a correction factor for the amount of slag will indeed be necessary. Roughly estimated from the limited number of experiments, doubling the weight of slag leads to a 50% longer ribbon. The amount of slag can be weighed

after cooling, so correcting the length after the measurement is feasible in an industrial set-up. A calibration is needed and expected to be possible, but from the limited amount of trials in this test series, it is not yet clear how many data points are needed for an accurate weight correction.

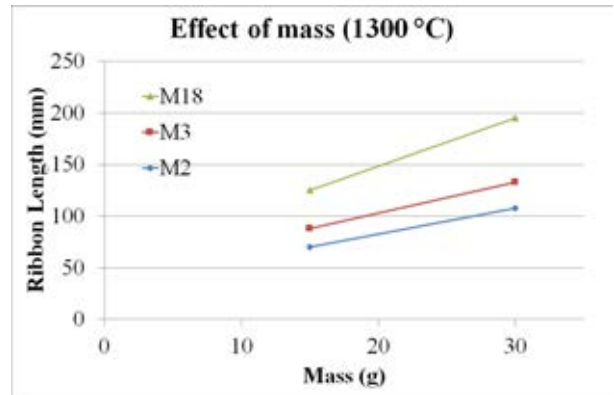


Figure 5: An increasing slag amount results in a longer ribbon

CFD model results

All results are compared to the base case as described earlier in the model specifications (Table 4). The flow of the base case is illustrated in Figure 6. The first frame, the red rectangle, illustrates the initial position of the slag phase. During the simulations, the slag will stream down the plate and form the slag ribbon. The last frame illustrates how the final slag ribbon looks like. This shape agrees with the experimental observed solidified slag ribbons. During the simulation, the temperature decreases, due to the contact with the steel plate. Consequently, the viscosity increases. The velocity of slag slows down due to this increasing viscosity. This can also be observed in Figure 7. In this figure, the length evolution of three different calculations is compared, in which the temperature dependence of the viscosity is changed as shown in Figure 8. The steeper the dependency of the slag viscosity on the temperature, the faster the velocity of the slag decreases, resulting in a shorter ribbon.

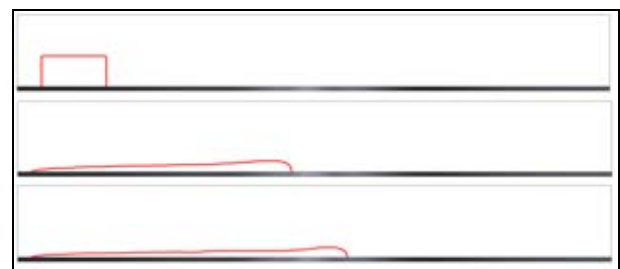


Figure 6: Contour evolution of the slag phase in the base case. From top to down: 0.0s, 0.5s and 1.0s

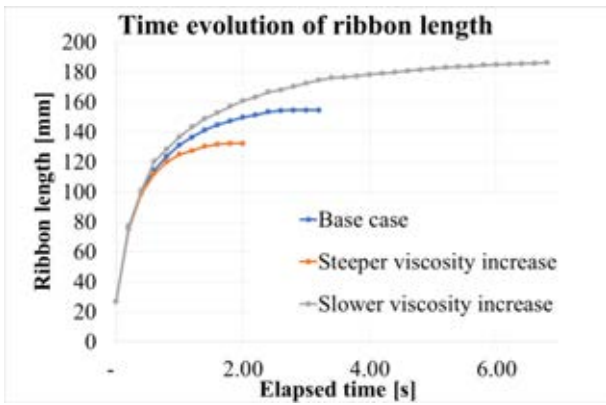


Figure 7: Time evolution of different temperature dependent cases

Figure 6 and Figure 7 prove that the maximum viscosity used in the UDF is sufficiently high to approximate the solidification. The ribbon length and shape of the slag phase all remain stable. For these length scales and forces, a liquid with a viscosity of 1000 Pa.s is practically solid.

Two types of parameters have been studied: set-up variations and material properties variations. The set-up variations include:

- increasing the inclination to 25°,
- increasing the initial temperature of the steel plate to 100 °C and 200 °C,
- increasing thickness of the steel plate to 5 mm,
- increasing the volume of slag by 59%, which corresponds to doubling a 3D cubic volume equally in all directions.

The material variations include:

- increasing/decreasing the slope of the Wayman-Frenkel relationship with a factor 2 while keeping the viscosity constant at 1300 °C (increased/decreased temperature dependency with the same start viscosity, dashed black lines in Figure 8),
- increasing the initial temperature of the slag to 1400 °C,
- doubling the initial viscosity with same temperature dependency (solid black line in Figure 8).

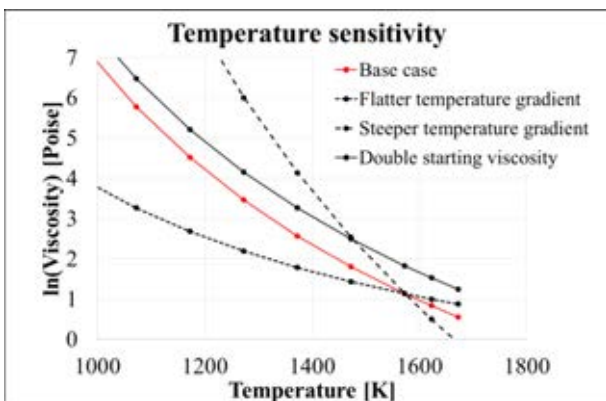


Figure 8: Temperature dependency of different cases. Red line is the base case scenario, the black lines represent changes in temperature dependency

The effect of the set-up parameters is summarized in Figure 9. By modelling the inclined plane, it can be concluded that the effect of both thickness and initial temperature of the plate are negligible for the final ribbon length. Consequently, doing sequential experiments, effectively increasing the initial temperature of the plate, will not largely influence the measured ribbon length. On the other hand, the angle of the plate and amount of material are to be calibrated for to obtain the actual viscosity from the ribbon length. In the model, the final length scales linearly with the amount of slag. This contradicts earlier experimental observations. This is due to neglecting the V-shape of the plate in the 2D model. In reality the system would react differently to an increasing amount of poured material. A 3D model seems prerequisite to correctly model the effect of a volume change.

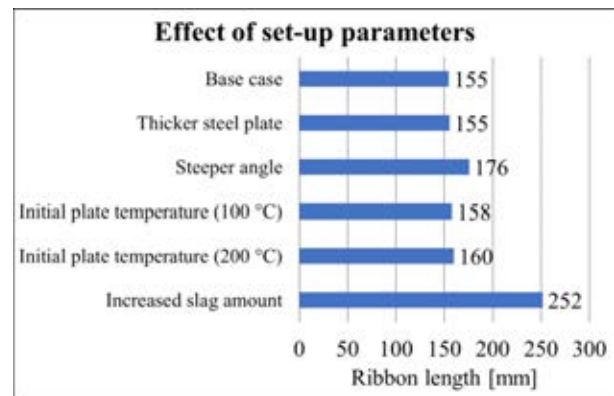


Figure 9: Effect of set-up parameters on ribbon length

The effect of the material property variations is summarized in Figure 10. The temperature dependency of the different cases is illustrated by Figure 8. Simulations with the same temperature dependency follow the experimentally observed linear relationship of Figure 4. However, Figure 10 indicates that the linear relationship between the final ribbon length and the viscosity is not depending on only the starting viscosity. In fact, the viscosity dependency on the temperature could cause serious deviations on the experimentally observed linear relationship.

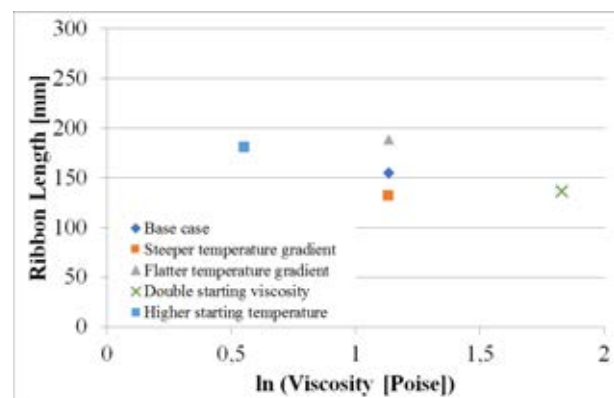


Figure 10: Effect of viscosity parameters on ribbon length

The inclined plane method therefore has the most comparative value if the temperature dependency for

different samples is similar. This will be the case in an industrial set-up where the same type of slag is always produced. This is also valid for the tested samples, for which the change in viscosity as a function of temperature is given in Figure 11. The Riboud model theoretically predicts the temperature dependency from the composition of the slag (Slag Atlas, 1995):

$$B = 31140 - 23896X_{CaO} - 46356X_{CaF_2} - 39159X_{Na_2O} + 68833X_{Al_2O_3} \quad (5)$$

with X being the molecular fraction of the different compounds. Consequently, the predicted values will change rather limited unless the molar fraction of aluminium is largely affected. For example, an increase of the molar fraction of alumina by 10% in the base case (with a decrease of calcium fluoride) will only lead to a change in temperature dependency of around 3%.

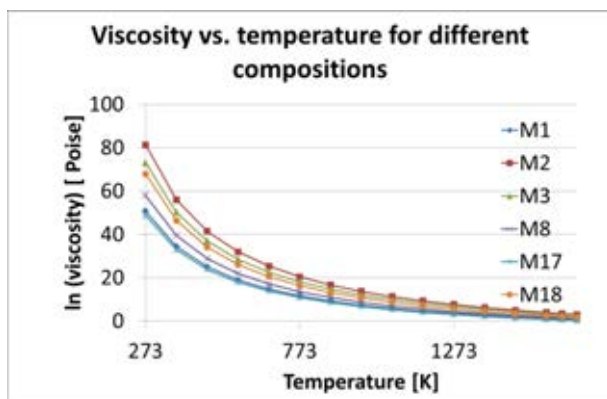


Figure 11: Viscosity dependencies on temperature for the different composition of the test campaign

Future Research

To validate the current model to the experimental data and to predict absolute ribbon lengths, a 3D model is necessary. Certain effects were neglected in the 2D model such as the stream of the slag to the centre of the gutter, a larger contact area with the steel plate, and a larger heat sink in the steel plate next to the sample. These effects make any quantitative and predictive model impossible when working in 2D.

Unfortunately, artefacts exist when working with high viscosity liquids in Fluent 18.0 with the current approach. The slag phase does not fully make contact with the metal plate, but a certain volume fraction of air remains present at the interface. This distorts the heat transfer. Currently this problem can also be recreated in 2D by increasing the viscosity. The effect is not present in the simulations used in this paper.

In Figure 12 a first result of the 3D model is given. Although the shape and movement of the slag look realistic, some optimisation steps are necessary to increase the credibility of the result, especially concerning the heat transfer at the boundary conditions.

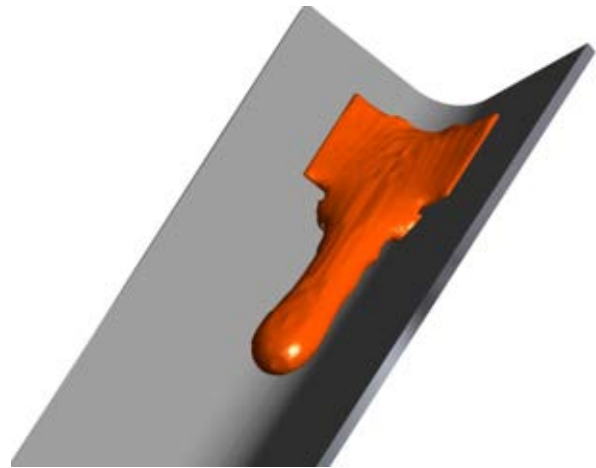


Figure 12: Illustration of 3D model

CONCLUSION

In this work, CFD was used to complement the outcome of a testing campaign to validate the inclined plane set-up as a technique to measure slag viscosity. CFD allowed to verify the influence of several material and set-up parameters which are difficult to test in lab environment. It was concluded that the inclined plane technique is a reliable and robust technique, which looks promising to be used in an industrial environment for fast measurements of viscosity. CFD showed that sequential testing does not pose too large deviations due to heating of the equipment and it proved that if the composition changes are not too large, a quantitative comparison of ribbon lengths and related viscosities is possible. Given the positive outcome of this study, further effort will be done to calibrate the measurement to make it available for industry.

ACKNOWLEDGEMENT

The authors would like to thank Kopila Gurung for performing the experiments.

REFERENCES

- ANSYS, (2017), "Fluent 18.0 documentation", Ansys Help 18.0.
- BALE, C.W., BELISLE, E., CHARTRAND, P., DECTEROY, S.A., ERIKSSON, G., CHERIBI, A.E., HACK, K., JUNG, I.H., KANG, Y.B., MELANCON, J. and PELTON, A.D., PETERSEN, S., ROBELIN, C., STANGSTER, J. and VAN ENDE, M.A. (2010-2016), "FactSage Thermochemical Software and Databases", *Calphad*, vol. 54, pp 35-53, 2016.
- CHEN, L., LI, S., JONES, P.T., MUXING, G., BLANPAIN, B. and MALFLIET, A. (2016), "Identification of magnesia-chromite refractory degradation mechanisms of secondary copper smelter linings", *Journal of the European Ceramic Society*, vol. 36, nr. 8, pp. 2119-2132.
- DEY, A. and RIAZ, S. (2012), "Viscosity measurement of mould fluxes using inclined plane test and development of mathematical model," *Ironmaking & Steelmaking*, vol. 39, nr. 6, pp. 391-397.

FERZIGER, J.H. and PERIC, M. (2002), “*Computational methods for fluid dynamics*”. Springer.

KEKKONEN, M., OGHBASILASIE, H. and LOUHENKILPI, S. (2012) “Viscosity models for molten slags”, School of chemical technology, Helsinki.

MILLS, K.C., HALALI, M., LÖRZ, H.P., KINDER, A., POMFRET, R. and WALKER, B. (1997), “A Simple Test for the Measurement of Slag viscosities”, *Molten Slags, Fluxes and Salts*.

REIS, B.H., BIELEFELDT, W.V. and VILELA, A.C.F., (2014), “Absorption of non-metallic inclusions by steelmaking slags – a review”, *Journal of Materials Research and Technology*, vol. 3(2) pp179-185.

SLAG ATLAS. 2nd edition, (1995), *Verlag Stahleisen GmbH*, Düsseldorf.

VERSTEEG, H.K. and MALALASEKERA, W., (2007), “An introduction to computational fluid dynamics: the finite volume method”, *Pearson Education Ltd*, Harlow.